BLACK OIL FORMULATION FOR THE MULTISCALE FINITE-VOLUME METHOD

S. H. LEE[1], C. WOLFSTEINER[1] AND H. A. TCHELEPI[2]

[1] Chevron Energy Technology Co., San Ramon, CA 094583, USA.
[2] Petroleum Engineering Dept., Stanford University, Stanford, CA 94305, USA.

Abstract

Most practical reservoir simulation studies are performed using the so-called black-oil model, in which the phase behavior is represented using solubilities and formation volume factors. We extend the multiscale finite-volume (MSFV) method to deal with nonlinear immiscible three-phase compressible flow in the presence of gravity and capillary forces (i.e., black-oil model). Consistent with the MSFV framework, we treat flow and transport separately and differently using a fully implicit sequential algorithm [6]. The pressure field is solved using an operator splitting algorithm. The general solution of the pressure is decomposed into elliptic, buoyancy-dominated, and capillary-dominated parts. The original MSFV framework is used to compute the elliptic component, which captures long range interactions in the pressure field. The effect of wells (sources/sinks) on the flow is represented as a particular solution. The methodology is demonstrated using black-oil examples of nonlinear compressible multiphase flow in strongly heterogeneous formations.

1. Introduction

Recent advances in multiscale methods have enhanced our ability to make predictions of flow and transport in highly detailed heterogeneous reservoir models. Jenny *et al.* [4, 5, 6] described in a series of papers a multiscale finite volume (MSFV) method for single-phase flow, adaptive IMPES (IMplicit pressure, Explicit Saturations), and fully implicit treatment of incompressible multiphase flow in heterogeneous porous media. The MSFV method solves flow and transport sequentially. To compute the fine-scale flow field, dual basis functions, which are solutions of local problems on the dual grid, are used to construct a global coarse-scale system of equations, which can be solved to obtain the global coarse grid pressure. The fine-scale total-velocity field is reconstructed using the primal basis functions. In the MSFV approach[5, 6], a block based Schwarz overlapping technique is used to solve the hyperbolic saturation equations (i.e., transport problem). The method has been proved to be accurate for strongly heterogeneous problems.

The black-oil formulation[1, 9] is often used to perform simulation studies in practice. In the black-oil model, three components, which are defined as fluid phases at standard (surface) conditions, are used to represent the fluid system. The hydrocarbon system is described using two pseudo components, namely oil and gas, and the third component represents water. The phase behavior of the fluid system is described using solubilities and

formation volume factors. Nonlinear immiscible three-phase (water, oil, gas) compressible flow with capillary and gravity effects can be modeled using the black-oil formulation. In this paper, we describe a MSFV black-oil simulator, which is an important step toward demonstrating the ability of the MSFV approach to deal with large-scale reservoir problems of practical interest.

The conservation equations of the three pseudo components are nonlinear. They are parabolic due to capillarity (three immiscible fluid phases) and compressibility (rock and fluids). However, in most settings, reservoir displacement processes are dominated by convection, so that the pressure field is nearly elliptic, while the saturation equations display nearly hyperbolic behavior. An operator splitting algorithm is devised to compute the pressure field. The general solution of the pressure is decomposed into elliptic, buoyancy-dominated, and capillary-dominated parts. The effect of wells (sources/sinks) on the flow field is represented as a particular solution.

Dual-grid basis functions, which are solutions to local problems on the dual grid, are used to assemble an upscaled transmissibility field on the coarse grid. Solution of this global system yields the coarse-scale pressure field. The fine-scale pressure can be reconstructed using the dual basis functions. The fine-scale saturation equations are then solved using the reconstructed fine-scale velocity field. In the saturation equation, a Schwarz overlap method is applied directly for a primal coarse cell with local boundary conditions. Direct construction of the velocity field and solution of the transport problem on the primal coarse grid allows for wide flexibility in accommodating additional physical mechanisms, such as compressibility, capillary pressure, and buoyancy. Note that the second set of basis functions described by Jenny *et al.* [4, 5] is not used here because the number of basis functions is rather large (27 basis functions in three dimensions).

2. Governing Equations and Discretized Formulation

The standard black-oil model includes two hydrocarbon phases (oil and gas) and one aqueous phase (water) with rock and fluid compressibility, gravity, and capillary pressure. The thermodynamic equilibrium between the hydrocarbon phases is described by the solubility of gas in the oil. The conservation equations are nonlinear due to the strong nonlinear character of the relative permeability and capillary pressure relations, high compressibility (especially of the gas), large density and viscosity differences, and phase appearance and disappearance. The governing black oil equations [1] are:

$$\frac{\partial}{\partial t}\left(\phi b_o S_o\right) = \nabla \cdot \left(b_o \lambda_o \cdot \left(\nabla p_o - g\rho_o \nabla z\right)\right) - q_o \tag{1}$$

$$\frac{\partial}{\partial t}\left(\phi b_w S_w\right) = \nabla \cdot \left(b_w \lambda_w \cdot \left(\nabla p_w - g\rho_w \nabla z\right)\right) - q_w \tag{2}$$

$$\begin{aligned} \frac{\partial}{\partial t}\left(\phi\left(b_g S_g + R_s b_o S_o\right)\right) &= \nabla \cdot \left(b_g \lambda_g \cdot \left(\nabla p_g - g\rho_g \nabla z\right)\right) - q_g \\ &+ \nabla \cdot \left(R_s b_o \lambda_o \cdot \left(\nabla p_o - g\rho_o \nabla z\right)\right) - R_s q_o, \end{aligned} \tag{3}$$

on the domain Ω, with boundary conditions on $\partial\Omega$. Here, $b_l = 1/B_l$ and $\lambda_l = \mathbf{k}k_{r_l}/\mu_l$ for phases $l = o, w, g$ (i.e., oil, water and gas). B_l denotes the formation volume factor of phase l (volume at reservoir conditions to volume at standard conditions). Similarly, S_l, k_{r_l}, μ_l, ρ_l denote, respectively, the saturation, relative permeability, viscosity, and density

of phase l. The well volumetric flow rate is q_l. The tensor $\mathbf{k}$ describes the permeability field, which is usually represented as a complex multiscale function of space that tends to be highly discontinuous in discrete representations. Porosity is denoted by ϕ, p_l is the pressure of phase l, g is gravitational acceleration, z denotes reservoir depth, and R_s is the solubility of gas in oil . In general, μ_l, ρ_l, B_l, R_s and ϕ are functions of pressure. The relative permeabilities, k_{r_l}, are strong functions of saturation.

The saturations are constrained by:

$$S_o + S_w + S_g = 1. \tag{4}$$

The three phase pressures p_w, p_o and p_g are related by two independent capillary pressure relationships, p_{cwo} and p_{cgo}. We choose the oil-phase pressure as a primary variable, p, and we derive the pressure equation. The semi-discrete form of each of Eqs. (1) , (2), and (3) is multiplied by α_o, α_w and α_g, respectively,

$$\alpha_o = 1/b_o^{n+1} - R_s^{n+1}/b_g^{n+1}, \quad \alpha_w = 1/b_w^{n+1}, \quad \text{and} \quad \alpha_g = 1/b_g^{n+1}, \tag{5}$$

and then added together. The resulting weighted sum removes the dependency of the current saturation level in the accumulation term. If one further linearizes the resulting equations around p^ν, the weighted sum represents the well-known pressure equation[1].

3. Multiscale Finite Volume Formulation

In the multiscale finite-volume (MSFV) algorithm of Jenny *et al.* [4, 5, 6], the basis functions are computed on the dual coarse grid, and the coarse-grid pressure is solved using upscaled transmissibilities. The basis functions allow for the reconstruction of the fine-scale pressure from the coarse scale pressure solution. In **Fig. 1** , the primal coarse grid ,Ω^c, and the dual coarse grid, Ω^d, are depicted.

The original MSFV algorithm [4] was designed to solve the elliptic pressure equation for incompressible flow in highly heterogeneous formations. The black-oil model, which accounts for compressibility and capillarity effects, yields a nonlinear parabolic pressure equation. However, compressibility and capillary effects are, in general, quite small. As a result, the pressure equation displays near-elliptic behavior. We design a multiscale algorithm for the pressure based on this observation. The pressure is decomposed into homogeneous and inhomogeneous parts. The homogenous (elliptic) component is denoted by p_h; the inhomogeneous part is composed of two contributions: gravity,p_g, and capillarity, p_p.

Following this procedure, the governing equations for the different pressure components can be written as

$$-\alpha_o\nabla\cdot\left(\lambda'^{\nu}_{o}\cdot\nabla p_h^{\nu+1}\right)-\alpha_w\nabla\cdot\left(\lambda'^{\nu}_{w}\cdot\nabla p_h^{\nu+1}\right)-\alpha_g\nabla\cdot\left(\lambda'^{\nu}_{g}\cdot\nabla p_h^{\nu+1}\right)=0 \tag{6}$$

$$-\alpha_o\nabla\cdot\left(\lambda'^{\nu}_{o}\cdot\nabla p_g^{\nu+1}\right)-\alpha_w\nabla\cdot\left(\lambda'^{\nu}_{w}\cdot\nabla p_g^{\nu+1}\right)-\alpha_g\nabla\cdot\left(\lambda'^{\nu}_{g}\cdot\nabla p_g^{\nu+1}\right)=RHS1 \tag{7}$$

$$\begin{aligned}-\alpha_o\nabla\cdot\left(\lambda'^{\nu}_{o}\cdot\nabla p_p^{\nu+1}\right)-\alpha_w\nabla\cdot\left(\lambda'^{\nu}_{w}\cdot\nabla p_p^{\nu+1}\right)-\alpha_g\nabla\cdot\left(\lambda'^{\nu}_{g}\cdot\nabla p_p^{\nu+1}\right)=\\ -\frac{C}{\Delta t}[(p_h+p_g+p_p)^{\nu+1}-(p_h+p_g+p_p)^{\nu}]+RHS2\end{aligned} \tag{8}$$

$$\begin{aligned}RHS1=&-\alpha_o\nabla\cdot\left(g\rho_o\lambda'^{\nu}_{o}\cdot\nabla z\right)-\alpha_w\nabla\cdot\left(g\rho_w\lambda'^{\nu}_{w}\cdot\nabla z\right)-\alpha_g\nabla\cdot\left(g\rho_g\lambda'^{\nu}_{g}\cdot\nabla z\right)\\&+\alpha_w\nabla\cdot\left(\lambda'_w\cdot\nabla p_{cwo}\right)^{\nu}+\alpha_g\nabla\cdot\left(\lambda'_g\cdot\nabla p_{cgo}\right)^{\nu}\end{aligned} \tag{9}$$

$$\begin{aligned}RHS2=&\frac{\phi^n}{\Delta t}\left(\left(\alpha_o+\alpha_g R_s^n\right)b_o^nS_o^n+\alpha_w b_w^nS_w^n+\alpha_g b_g^nS_g^n\right)-\frac{\phi^{\nu}}{\Delta t}\\&-\left(\alpha_o q_o^{\nu}+\alpha_w q_w^{\nu}+\alpha_g(q_g+R_s q_o)^{\nu}\right)\end{aligned} \tag{10}$$

$$\begin{aligned}C=&\frac{\partial\phi}{\partial p}\Big|^{\nu}-\phi^n\left(\frac{\partial\alpha_o}{\partial p}\Big|^{\nu}b_o^nS_o^n+\frac{\partial\alpha_w}{\partial p}\Big|^{\nu}b_w^nS_w^n+\frac{\partial\alpha_g}{\partial p}\Big|^{\nu}(b_g^nS_g^n+R_s^nb_o^nS_o^n)\right)\\&+\Delta t\left(\frac{\partial\alpha_o q_o}{\partial p}\Big|^{\nu}+\frac{\partial\alpha_w q_o}{\partial p}\Big|^{\nu}+\frac{\partial\alpha_g(q_g+R_s q_o)}{\partial p}\Big|^{\nu}\right)\end{aligned} \tag{11}$$

$$\lambda'^{\nu}_{o}=b_o^{\nu}\lambda_o^{\nu},\quad \lambda'^{\nu}_{w}=b_w^{\nu}\lambda_w^{\nu},\quad \text{and}\quad \lambda'^{\nu}_{g}=b_g^{\nu}\lambda_g^{\nu}+R_s^{\nu}b_o^{\nu}\lambda_o^{\nu}. \tag{12}$$

The total solution p is $p_h+p_g+p_p$, where p_p is the particular solution due to the accumulation term and wells (sources/sinks). The elliptic pressure component, Eq. (6), can be computed using the original MSFV method of Jenny *et al.* [4].

3.1. **Homogeneous Pressure Solution.** The MSFV[4] yields an accurate fine scale pressure solution by employing a coarse grid. The reconstructed fine-scale field is obtained using the coarse-scale pressure solution and the local basis functions. Quite recently, Lunati and Jenny [8] derived a MSFV method for compressible multiphase flow. Our scheme is very similar to their third algorithm, but without explicit computation of the average formation volume factors in the coarse grid.

The dual basis functions are used to assemble a coarse-scale transmissibility field, which is used to compute the coarse-scale pressure, p_i^c. The dual basis function Θ_j^i, for example, is the local solution of Eq. (6):

$$\alpha_o\nabla\cdot\left(\lambda'^{\nu}_{o}\cdot\nabla\Theta_j^i\right)+\alpha_w\nabla\cdot\left(\lambda'^{\nu}_{w}\cdot\nabla\Theta_j^i\right)+\alpha_g\nabla\cdot\left(\lambda'^{\nu}_{g}\cdot\nabla\Theta_j^i\right)=0\quad\text{on}\quad\Omega_j^d. \tag{13}$$

3.2. **Inhomogeneous Solution with Gravity and Capillary Pressure.** As shown in Eq. (7), the inhomogeneous solution, p_g, accounts for gravity and capillary forces. Due to the complexity of the fractional flow function in the presence of gravity, the potential field cannot be represented by a simple superposition of the basis function. Lunati [7] proposed an efficient algorithm to compute p_g by splitting it into two parts. The first part is represented by the original basis functions; the second part is a correction term based on solving a local problem that accounts for buoyancy effects. Following Lunati's

approach [7], we decompose p_g into two parts:

$$p_g = p_g^a + p_g^b = \sum_i \Theta_j^i p_g^{c,i} + p_g^b \ \text{ in } \ \Omega_j^d. \tag{14}$$

Note that in the dual coarse grid Ω_j^d, p_g^a is represented by a weighted linear combination of the coarse grid pressure, $p_g^{c,i}$, where the weights are given by the basis functions. The correction term, p_g^b is obtained from Eq. (7):

$$-\alpha_o \nabla \cdot \left(\lambda'^{\nu}_o \cdot \nabla p_g^b\right) - \alpha_w \nabla \cdot \left(\lambda'^{\nu}_w \cdot \nabla p_g^b\right) - \alpha_g \nabla \cdot \left(\lambda'^{\nu}_g \cdot \nabla p_g^b\right) = RHS1 \ \text{ in } \ \Omega^d, \tag{15}$$

where solutions of reduced problems consistent with Eq. (15) serve as boundary conditions. This localization assumption to compute p_g^b is analogous to the one used to construct the dual basis function in the absence of gravity effects. Lunati[7], who proposed this approach, shows its effectiveness in resolving the fine-scale structures of complex heterogeneous problems where buoyancy plays an important role.

Substituting Eq. (14) into the governing equation, Eq. (7), and applying Green's theorem for the coarse-grid operation [7], it can be shown that the solution from p_g^b becomes an additional source/sink for the coarse-grid operator. Once p_g^b is computed, we can compute the coarse grid pressure p_g^c by the coarse grid transmissibility described in the previous section and the additional source term from p_g^b. The p_g^c, as a result, does not have to be calculated separately. We can calculate the coarse grid block pressure together with other source/sink and accumulation terms, which are treated in the next section.

3.3. **Particular Solution with Wells and Accumulation Terms.** In addition to capturing the effects of the presence of sources/sinks (wells) in the domain, the particular solution, p_p, given by Eq.(8), accounts for compressibility effects on the accumulation terms. Accurate modeling of wells is crucial for practical use of any reservoir simulator. A multiscale treatment of wells is described by Wolfsteiner *et al.* [10]. That framework allows for modeling wells operated under constant-rate or constant-pressure constraints and that penetrate one or multiple fine cells. The idea is based on first computing and removing the local near-singular pressure distribution in the vicinity of the well, and then superposing this effect to a smoothly varying background solution computed using the original multiscale finite-volume method[4]. To simplify the derivation of the inhomogeneous solution here, wells are represented as distributed fine-scale source terms in the coarse-grid containing the well, as in Jenny *et al.* [4].

The coarse-grid transmissibility is obtained from the homogeneous (elliptic) component. If the coarse-grid transmissibility field does not change for the particular solution with sources/sinks and accumulation terms, the coarse grid pressure is computed directly. With the coarse-grid transmissibility approximation, one can write a mass balance equation for each coarse cell Ω_i^c ($i \in \{1, ..., M\}$), and the entire system can be solved for the coarse pressure ($p_i^c = p_{p,i}^c + p_{g,i}^c$). Once the coarse-grid pressure is computed, the fine-grid pressure field in the dual grid can be obtained using the basis functions.

3.4. **Fine-Scale Pressure and Velocity Fields.** Jenny *et al.* [4, 5] found that the fine-grid velocity field constructed using the coarse-grid pressure p_i^c and the dual basis functions Θ_j^i suffers from local mass balance errors at the interfaces between dual coarse

cells. They proposed a second set of (primal) basis functions to construct a conservative velocity field. Using the fine-scale fluxes obtained from the dual basis functions as boundary conditions when computing the fine-scale basis functions is crucial for ensuring that the reconstructed fine-scale velocity field is conservative. Even though an adaptive method can be employed to eliminate unnecessary computation of the second set of basis functions, the large number of such basis functions does not guarantee that this approach is numerically more efficient than direct computation of the velocity and saturation fields every time step, or iteration. Furthermore, this direct approach does not require strict linearity of the governing equation and can be easily extended to include many nonlinear effects. Examples include compressibility, solubility, and capillary pressure. We employ the direct approach here. From the coarse grid pressure solution and the dual basis functions, the fine grid pressure field in a primal coarse grid is constructed. Neumann boundary conditions on the primal coarse grid are computed, and then the fine scale velocity is computed for the local problem of interest.

3.5. **Sequential Fully Implicit Algorithm and Adaptive Computation.** The algorithm comprises two major steps. First the phase velocities are obtained from solving the pressure equation using the MSFV method. Then, the transport equation is solved on the fine grid using the reconstructed fine-scale phase velocity field. A Schwarz overlap method is used to solve the saturation equations.

The MSFV approach can be easily adapted to a sequential fully implicit treatment[6]. The MSFV implementation allows for performing an IMPES, traditional sequential[1], or a fully implicit scheme. Here, the full nonlinear transmissibility terms at the new time step level are retained so that stability is guaranteed [5]. The converged solution using this sequential approach should be identical to the solution obtained using the simultaneous solution strategy, which is usually used to deal with the coupled fully implicit system.

The MSFV is well suited for adaptive computation, which can lead to significant gains in computational efficiency. The most expensive part of the algorithm is the computation of the dual basis functions. In general, this is performed every iteration due to changes in the saturation (mobility) field. As discussed in Jenny *et al.* [5], an adaptive scheme can be used to update the dual basis functions. Since the basis functions are constructed with local support, the change of the total mobility is used to decide when and where to update the basis functions in the domain.

4. Numerical Examples

4.1. **Waterflood in Linear Geometry.** The first example is a two-dimensional model from one layer of the Tenth SPE Comparative Solution Project [2]. The model is discretized using 110×60 fine cells. A uniform coarse grid of 22×6 is used. The permeability distribution is shown in **Fig. 2** (a). The physical properties of the black-oil model include compressible three-phase fluids (i.e., oil, water, and gas). The pressure dependence of the densities is described using formation volume factors, and the phase equilibrium between the oil and gas phases is described using the solution gas-oil-ratio [3]. The model is initialized with oil ($S_o = 1$) and constant pressure (4000 psia). At $t = 0$, water is injected at a constant pressure of 5000 psia from the left side; the right boundary is maintained at

2000 psia. This numerical example is a challenging test due to the large pressure drops applied to fluids with large variation in compressibility as well as high gas solubility.

In Fig. 2 the results from the MSFV simulator and fine-scale reference simulations are depicted at 50 days. Because gas compressibility is two to three orders of magnitude larger than that of either oil or water, a large pressure drop occurs at the boundary of the oil phase above the bubble-point pressure and the mixed (oil and gas) phase below the bubble point. This sharp pressure drop is demonstrated clearly in Fig. 2 (b). The figure indicates that the saturation distributions of water and gas obtained from the MSFV simulation are in good agreement with reference fine-scale solutions.

4.2. **Cross Section with Two Wells.** The second example is a cross sectional model of a two-phase displacement with gravity. The permeability is homogeneous, $k = 100$ md, and the porosity is $\phi = 0.2$. The fluid compressibilities are 2.37×10^{-4} psi^{-1} for water and 1.37×10^{-4} psi^{-1} for oil. The viscosities and densities are 1 cp and 1 g/cc for water and 2 cp and 0.5 g/cc for oil, respectively. A coarse grid of 5×5 was constructed from the fine grid, which is 25×25.

Water is injected at constant rate from the bottom left corner displacing the oil toward the producer located at the top left corner. The overall fluid movement is upward. **Fig. 3** shows water saturation contours (from $S_w = 0.1$ to $S_w = 0.9$) at 0.21, 0.42 and 0.64 PVI (pore volume injected/total pore volume) from the multiscale method and reference fine-scale solutions. The saturation contours indicate downward movement of the heavy fluid (water). For all three snapshots, the saturation contours from the MSFV approach are in excellent agreement with those from the fine-scale reference simulation.

5. Conclusions

We developed a multiscale finite-volume (MSFV) method for the black oil formulation of multiphase flow and transport in heterogeneous porous media. The black oil formulation, which involves three-phase flow with rock and fluid compressibility, gravity, and capillary effects, is widely used in practical field-scale simulations. Our approach is extends the sequential fully implicit MSFV method [6] to nonlinear three-phase compressible flow with mass transfer expressed using solubilities. An operator splitting algorithm is devised to compute the fine-scale pressure field. The black-oil MSFV method extends our ability to deal with large-scale problems of practical interest. The treatment ensures that the nonlinearity due to fluid properties, gravity, and capillarity can be resolved by a localization assumption for the boundary conditions. We included two numerical examples to demonstrate the method. These examples show clearly that the MSFV scheme yields results that are in very good agreement with reference fine-grid solutions.

Although the numerical efficiency of this new black-oil MSFV simulator has not been fully examined, the numerical efficiency gains shown in Jenny *et al.*[5, 6] are expected to still hold. This is because all the nonlinearities due to the presence of compressibility, gravity and capillary pressure are resolved locally. A detailed analysis of the numerical efficiency for large-scale heterogenous problems of practical interest will be presented in a future publication.

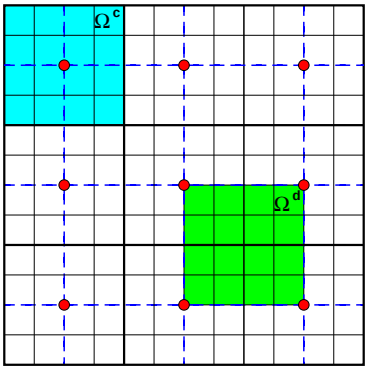

FIGURE 1. Primal coarse grid and dual coarse grid

Acknowledgment: We thank P. Jenny and I. Lunati for many constructive discussions and suggestions during the course of this work. This project was funded by the Chevron/Schlumberger Intersect Alliance Technology.

REFERENCES

1. K. Aziz and A. Settari, *Petroleum reservoir simulation*, Elsevier Applied Scientific Pub., 1979.
2. M. A. Christie and M. J. Blunt, *Tenth spe comparative solution project: A comparison of upscaling techniques*, SPERE **4** (2001), no. 4, 308–17.
3. B.C. Craft, , and M. F. Hawkins, *Petroleum reservoir engineering*, Prentice-Hall, Inc., 1959.
4. P. Jenny, S. H. Lee, and H. A. Tchelepi, *Multi-scale finite-volume method for elliptic problems in subsurface flow simulation*, J. Comp. Phys. **187** (2003), 47–67.
5. _____, *Adaptive multiscale finite volume method for multi-phase flow and transport*, Multiscale Model. Simul. **3** (2004), 50–64.
6. _____, *An adaptive fully implicit multi-scale finite-volume algorithm for multi-phase flow in porous media*, J. Comp. Phys. (In Press, 2006).
7. I. Lunati, *Multi-scale finite-volume method for multi-phase flow with gravity*, Technical report, Chevron/Schlumberger Technical Alliance, 2005.
8. I. Lunati and P. Jenny, *Multi-scale finite-volume method for compressible multi-phase flow in porous media*, submitted to J. Comp. Phys. (In Press, 2006).
9. D. W. Peaceman, *Fundamentals of numerical reservoir simulation*, Elsevier Scientific Pub., 1977.
10. C. Wolfsteiner, S. H. Lee, and H. A. Tchelepi, *Modeling of wells in the multiscale finite volume method for subsurface flow simultion*, Multiscale Model. Simul. (Submitted July, 2005).

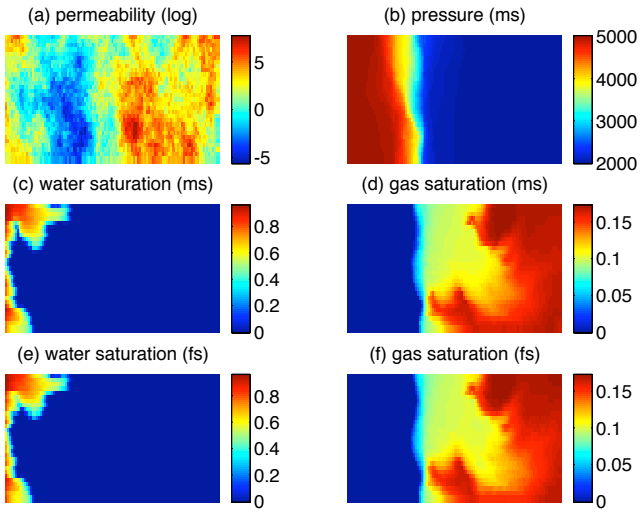

FIGURE 2. Two-dimensional waterflood from left to right at 50 days: (a) logarithm of permeability, (b) pressure from MSFV, (c) S_w from MSFV,(d) S_g from MSFV, (e) S_w from reference fine-scale simulation, (f) S_g from reference fine scale simulation.

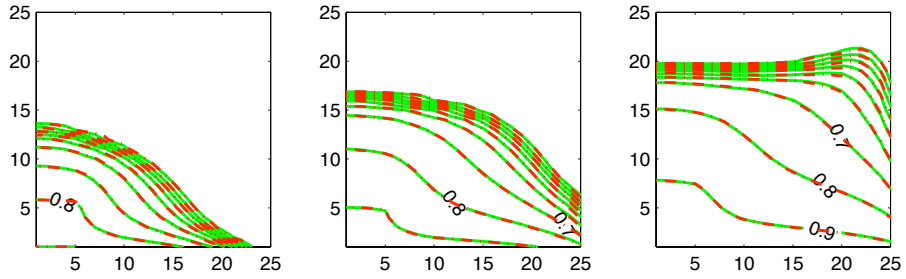

FIGURE 3. Contour lines of water saturation: (a) 0.21 PVI (b) 0.42 PVI and (c) 0.64 PVI. Solid contours represent multiscale, and dashed contours represent reference fine-scale results.